Published in final edited form as:
J Cancer Res Clin Oncol. 2013 June ; 139(6): . doi:10.1007/s00432-013-1398-0.

Delivery of the co-expression plasmid pEndo-Si-Stat3 by attenuated *Salmonella* serovar *typhimurium* for prostate cancer treatment

Xin Li,
Department of Pathophysiology, Prostate Diseases Prevention and Treatment Research Center, Norman Bethune Medical School, Jilin University, Xinmin Street, Changchun 130021, People's Republic of China

Yang Li,
Department of Pathophysiology, Prostate Diseases Prevention and Treatment Research Center, Norman Bethune Medical School, Jilin University, Xinmin Street, Changchun 130021, People's Republic of China

Bo Wang,
Department of Pathophysiology, Prostate Diseases Prevention and Treatment Research Center, Norman Bethune Medical School, Jilin University, Xinmin Street, Changchun 130021, People's Republic of China

Kun Ji,
Department of Pathophysiology, Prostate Diseases Prevention and Treatment Research Center, Norman Bethune Medical School, Jilin University, Xinmin Street, Changchun 130021, People's Republic of China

Zuowen Liang,
Department of Pathophysiology, Prostate Diseases Prevention and Treatment Research Center, Norman Bethune Medical School, Jilin University, Xinmin Street, Changchun 130021, People's Republic of China

Baofeng Guo,
Department of Pathophysiology, Prostate Diseases Prevention and Treatment Research Center, Norman Bethune Medical School, Jilin University, Xinmin Street, Changchun 130021, People's Republic of China

Jiadi Hu,
Department of Oncology and Diagnostic Sciences, School of Dentistry, University of Maryland, Baltimore, MD, USA

Di Yin,
Department of Pathophysiology, Prostate Diseases Prevention and Treatment Research Center, Norman Bethune Medical School, Jilin University, Xinmin Street, Changchun 130021, People's Republic of China

Yanwei Du,

Correspondence to: Ling Zhang, zhangling3@jlu.edu.cn.

Xin Li and Yang Li contributed equally to this work.

Conflict of interest The authors declare no conflicts of interest.

Department of Pathophysiology, Prostate Diseases Prevention and Treatment Research Center, Norman Bethune Medical School, Jilin University, Xinmin Street, Changchun 130021, People's Republic of China

Dennis J. Kopecko,
Laboratory of Enteric and Sexually Transmitted Diseases, Center for Biologics Evaluation and Research, Food and Drug Administration, Bethesda, MD, USA

Dhananjaya V. Kalvakolanu,
Department of Microbiology and Immunology, Molecular Biology Program, Greenebaum Cancer Center, University of Maryland School Medicine, Baltimore, MD, USA

Xuejian Zhao,
Department of Pathophysiology, Prostate Diseases Prevention and Treatment Research Center, Norman Bethune Medical School, Jilin University, Xinmin Street, Changchun 130021, People's Republic of China

Deqi Xu, and
New Vaccine National Engineering Research Center, Beijing 100024, People's Republic of China

Ling Zhang
Department of Pathophysiology, Prostate Diseases Prevention and Treatment Research Center, Norman Bethune Medical School, Jilin University, Xinmin Street, Changchun 130021, People's Republic of China

Deqi Xu: dqxujl@gmail.com; Ling Zhang: zhangling3@jlu.edu.cn

Abstract

Objectives—To investigate the therapeutic utility of an attenuated bacterium carrying a plasmid that co-expresses Endostatin, an inhibitor of tumor neovasculogenesis, and a shRNA that targets Stat3 to suppress prostate cancer growth.

Methods—Plasmid pEndo-Si-Stat3 was constructed and introduced into an attenuated strain of *Salmonella enterica* serovar *typhimurium*. The resultant recombinant bacterium was used as a vector to deliver the plasmid to tumor cells growing in vivo. Tumor-associated gene and protein expression changes were measured by using RT-PCR and Western blot analyses. Expression of Endostatin in tumor tissue was detected by ELISA. The presence of vector bacteria in tissues was monitored and tumor destruction was assessed by using TUNEL and H&E staining assays.

Results—Bacterially delivered pEndo-Si-Stat3 decreased Stat3 levels and increased Endostatin expression in mouse tumors, resulting in a significant suppression of tumor growth ($P < 0.01$). Expression of Bcl-2 and PCNA was down-regulated and Caspase3 expression was up-regulated to promote apoptosis of tumor cells.

Conclusions—Successful delivery by attenuated *Salmonella* of the combination therapeutic plasmid simultaneously knocked down the expression of Stat3 and resulted in over-expression of Endostatin, which synergistically inhibited prostate cancer growth.

Keywords

Prostate cancer; Stat3; Endostatin; Attenuated *Salmonella typhimurium*

Introduction

Prostate cancer is the most common cancer among men (Kamangar 2012). With the worldwide expansion of aging society, the incidence and mortality of prostate cancer are increasing, and better therapies are urgently needed. Following recent advances in cell and

molecular biology, cancer gene therapy is poised to move forward with promising new targets.

RNA interference (RNA*i*), a mechanism by which double-stranded RNAs mediate sequence-specific gene silencing, has provided a new tool in the fight against cancer (Oshima et al. 2003). Our previous studies demonstrated that delivery of therapeutic plasmids expressing specific anti-tumor siRNAs (targeting Stat3, MDM2, VEGF or survivin) and tumor suppressor proteins (e.g., GRIM-19 and p53) by attenuated *Salmonella* significantly reduces average tumor volume and exerts synergistic anti-tumor effects that are more effective than other delivery methods (Shao et al. 2010; Xu et al. 2009; Zhang et al. 2008, 2007). *Salmonella typhimurium* specifically survive in macrophages that are involved in targeting tumor tissues. Furthermore, *Salmonella* are facultative anaerobes that grow in tumors, in which hypoxic microenvironments exist. As a model delivery system for mice, we have utilized the *phoP/phoQ* deletion–attenuated *S.typhimurium* carrying a plasmid designed to synthesize siRNAs and tumor suppressor proteins under the control of eukaryotic gene promoters.

Stat3 is a member of the Signal Transducers and Activators of Transcription family of factors. Chronic activation of this pathway leads to abnormal cell proliferation and malignant transformation (Bromberg et al. 1999). Hyperactive Stat3 promotes the expression of downstream targeted genes, such as *VEGF*, *Cyclin D1*, *Cyclin D2*, *c-Myc*, *P53*, *Bcl-X_L*, *Bcl-2*, *Mcl-1* and *Survivin*. Furthermore, this pathway has been identified as an effective molecular target for treatment for a variety of human tumors (Buettner et al. 2002; Nam et al. 2005).

Angiogenesis is the growth of new capillaries from preexisting blood vessels, and it is a crucial step in tumor evolution (Beck et al. 2002). Among many angiogenesis inhibitors that have been investigated and considered for potential cancer therapy, Endostatin is the most potent inhibitor of tumor growth in animals and in clinical trials (Ryan and Wilding 2000). Endostatin specifically affects endothelial cells, especially microvascular endothelial cells (Huang et al. 2001; Shichiri and Hirata 2001), and has been shown to inhibit angiogenesis in nasopharyngeal, cervical, colon, breast, liver and prostate cancer and other solid tumors (Li et al. 2008; Liu et al. 2007; Passey 2006).

While gene therapy is a promising technology, its application is hampered by lack of site-specific delivery tools. We have constructed a bicistronic plasmid that allows the simultaneous expression of both Endostatin and a Stat3-specific siRNA. We report here the therapeutic utility of a bacterial vector (i.e., attenuated *Salmonella*) used to co-deliver pEndo-Si-Stat3 to prostate tumor-bearing mice to test its effects on tumor growth.

Materials and methods

Plasmid construction

The plasmid pEgγ-ss Endostatin was provided by Dr. Li Xiujuan. The expression plasmid pH1-Si-Stat3 was constructed as described previously (Zhang et al. 2008). To make the combined construct, the Endostatin-coding fragment from pEgγ-ss Endostatin was removed following digestion with *Kpn*I. The pH1-Si-Stat3 plasmid was digested with *Bgl*II and *Nru*I to obtain the H1-Si-Stat3 fragment. The Endostatin and H1-Stat3 fragments were then ligated to pcDNA3.1 to construct the co-expression *pEndo-Si-Stat3* plasmid. The expected DNA sequence was verified for the combination plasmid pEndo-Si-Stat3.

Bacteria and cell culture

The attenuated *S. typhimurium phoP/phoQ* null strain LH430 was kindly provided by Hohmann et al.(1996). The RM-1 mouse prostate cancer cell line was obtained from the Shanghai Institute of Cellular Research, China. These cells were grown in 1,640 medium (Hyclone, Logan, UT) with 10 % fetal bovine serum.

Establishment of the mouse tumor implantation model

Male C57BL/6 mice were purchased from the experimental animal center of Jilin University. The mice were inoculated subcutaneously with RM-1 prostate cancer cells (6×10^6 cells/150 μl) which were allowed to grow for 5 days. Tumors were removed and were cut into 1-mm^3 blocks and then implanted into the right flanks of C57BL/6 mice. After 5 days, the mice were randomly divided into 5 groups ($n = 8$). On day 12, following tumor implantation, each group of mice was injected intravenously with one of the indicated agents: (1) PBS (Mock), (2) attenuated *Salmonella* (5×10^7 cfu/100 μl) with either plasmid pSi-Scramble, or (3) *pEndostatin*, or (4) pSi-Stat3, or (5) pEndo-Si-Stat3. Tumor volume was measured every 4 days. On day 32, all mice were killed, and tumor tissues from each group were excised for follow-up experiments.

Semi-quantitative RT-PCR and Western blot

The expression of Endostatin, Stat3 and Stat3-regulated target genes (*Bcl-2* and *VEGF*) was quantified using semi-quantitative reverse transcription PCR (RT-PCR). RNA (5 μg) was reverse-transcribed into cDNA. The indicated transcripts were PCR-amplified using gene-specific primers. Band intensities were quantified and normalized to those of *GAPDH*, an internal control for these experiments.

Proteins (30 μg) from the samples were used for Western blot analyses. The primary antibodies used for Western blotting were against Endostatin (Biosynthesis, Beijing), Stat3, p-Stat3, Bcl-2 (Boster, Wuhan) and VEGF (Santa Cruz Biotechnology, USA). The secondary antibodies were purchased from Santa Cruz Biotechnology (USA).

Immunohistochemistry

Immunohistochemistry was performed as described elsewhere (Zhang et al. 2007). Tissue sections were immunostained with Stat3, CD34, PCNA or Caspase3 antibodies (Santa Cruz Biotechnology Inc., Santa Cruz, CA). Diaminobenzidine (DAB) was used for color development. CD34 is indicated in brown and is expressed in the cytoplasm of vascular endothelial cells. The microvessel density (MVD) count method refers to the Weidner correction method (Weidner et al. 1992). PCNA expression was assessed as a measure of the rate of cell proliferation. Positive or negative reactions were determined in five random fields of each sample with image processing software Image-Pro Plus 6.0.

TUNEL assay

The DeadEnd™ Fluorometric TUNEL System was used to measure the fragmented DNA of apoptotic cells. Apoptosis in tissues was detected by TUNEL assays following the manufacturer's instructions (Promega, USA). TUNEL-positive cells were indicated by green fluorescence.

Statistical analyses

Origin 7.5 (OriginLab Corp., Northampton, MA) laboratory data analysis software and image processing software (Image-Pro Plus 6.0) were used to quantitate data. All data were expressed as mean ± SD. One-way analysis of variance was employed with SPSS version

13.0 software to determine the significance of differences across treatment groups, and $P < 0.05$ was considered significant.

Results

Effects of the co-expression plasmid *pEndo-Si-Stat3* on the expression of Stat3 and Endostatin in tumors

To determine the effects on tumor cells of the co-expression plasmid pEndo-Si-Stat3, semi-quantitative RT-PCR, Western blot assay and ELISA were used to analyze Stat3 and Endostatin expression in tumors. The Stat3 mRNA (Fig. 1a, b) and protein levels (Fig. 1c, d) decreased in the pSi-Stat3 and pEndo-Si-Stat3 groups compared to the Mock and pSi-Scramble groups. In contrast, the Endostatin mRNA (Fig. 1a, b) and protein levels (Fig. 1c, d) increased in the pEndostatin and pEndo-Si-Stat3 groups compared with the Mock and pSi-Scramble groups. Thus, simultaneous suppression of Stat3 and over-expression of Endostatin were achieved successfully.

Delivery of pEndo-Si-Stat3 using attenuated *Salmonella* inhibits the growth of prostate tumors in mice

To test the anti-tumor efficacy of pEndo-Si-Stat3, a syngeneic murine prostate tumor RM-1 was established as described in “Materials and methods” section. On day 12, each group of tumor-bearing mice was injected intravenously with attenuated *Salmonella* carrying various plasmids expressing combinations of Endostatin and Si-Stat3. Tumor volume was monitored until day 32, when all mice were killed to collect tumor samples.

To determine whether the attenuated *S. typhimurium* delivered the treatment plasmids preferentially to tumor tissue, we monitored the kinetics of bacterial distribution in the tumor and other body tissues. On day 1, large numbers of attenuated *Salmonella* were found in tumor, liver and spleen tissues. Bacterial numbers remained significantly elevated in tumors, but declined in the liver and spleen by day 7. On day 14, bacterial accumulation was observed predominantly in tumor tissue and, to a far lesser extent, in the liver and spleen. Bacteria were not detected in other organs (data not shown).

Next, the potential therapeutic effect of bacteria carrying a plasmid expressing both Si-Stat3 and Endostatin on prostate tumor growth was examined in tumor-bearing mice. Tumor growth was monitored from the 4th day until the 32nd day after bacterial delivery of the treatment plasmids. Tumor size in the Mock or pSi-Scramble groups increased rapidly from days 4 to 16 and continued to increase from days 16 to 32 (Fig. 2b). Tumors in the pEndo-Si-Stat3 group grew more slowly and were significantly smaller than those in either the pEndostatin or pSi-Stat3 groups. Tumors were removed for the analysis of tumor size and weight on day 32. Figure 2 shows that the individual tumors from the pEndo-Si-Stat3 group were significantly smaller than those from the pSi-Scramble group ($P < 0.01$). Tumor weights were also significantly decreased in the pEndo-Si-Stat3, pSi-Stat3 or pEndostatin groups compared to the Mock or pSi-Scramble groups. To further quantitate the treatment-mediated change in tumor growth, we measured PCNA expression in the tumors. Compared to the control, PCNA expression in the pEndostatin, pSi-Stat3 and pEndo-Si-Stat3 groups was markedly decreased, with the largest change being observed in the pEndo-Si-Stat3 group. The proliferation index (PI) was 6.2 % ± 1.7 in the pEndo-Si-Stat3 group, which was significantly lower than in the Mock or pSi-Scramble groups ($P < 0.01$, Fig. 2d, e).

Inhibition of tumor angiogenesis as assessed by CD34 and VEGF expression in tumors

To determine whether the inhibition of tumor growth was accompanied by decreased tumor angiogenesis, tumor samples were analyzed by immunohistochemical analysis for CD34 and

by RT-PCR and Western blot analyses for VEGF. When compared to the Mock or pSi-Scramble groups, the expression of CD34 in tumors was robustly suppressed in the pEndostatin, pSi-Stat3 and pEndo-Si-Stat3 groups, with lowest levels in the pEndo-Si-Stat3 group (Fig. 3a, b). The levels of both *VEGF* mRNA (Fig. 3c, d) and protein (Fig. 3e, f) were strongly suppressed in the pEndostatin, pSi-Stat3 and pEndo-Si-Stat3 treatment groups, compared to the Mock or pSi-Scramble groups.

Effects of the co-expression plasmid *pEndo-Si-Stat3* on tumor cell death and the expression of Stat3 target genes

Since suppression of growth signals is accompanied by activation of apoptosis, we analyzed apoptosis in these tumors by immunohistochemical staining for Caspase3 (400×) and by TUNEL staining (Fig. 4a). Histological examination with H&E staining revealed a few focal areas of necrotic cells along with tissue disorganization in the pEndostatin, pSi-Stat3 and pEndo-Si-Stat3 treatment groups (Fig. 4a). Expression of activated Caspase3 (Fig. 4a, b) was markedly elevated in tumors treated with pEndo, pSi-Stat3 or pEndo-Si-Stat3. TUNEL assays showed increased numbers of apoptotic cells in the pEndostatin, pSi-Stat3 and pEndo-Si-Stat3 groups when compared to the control groups, with the greatest increase occurring in the pEndo-Si-Stat3 group. Apoptosis was evidenced by sparsely dispersed chromatin and necrotic tissues (Fig. 4a). The apoptosis index was highest in the pEndo-Si-Stat3 group (51.2 % ± 7.2), which was significantly higher than that in the control group (Fig. 4c). pSi-Stat3 also markedly increased the apoptosis index.

Constitutively active Stat3 alters the expression of several genes involved in apoptosis, including *CASP3* and *BCL-2* (Real et al. 2002). Therefore, we examined the expression of these genes in tumors treated with different plasmids. The expression of *Bcl-2* (Fig. 4d–g) mRNA and protein was examined by RT-PCR and Western blot analysis, respectively. We also observed that the expression of Caspase3 protein was greatly increased in tumors treated with plasmids containing Si-Stat3, versus the Mock or Scramble controls. In contrast, the expression of Bcl-2 protein was strongly diminished in tumors treated with *pSi-Stat3* and *pEndo-Si-Stat3*.

Discussion

Our long-term goal is to develop tumor-specific therapies using a tumor-targeting bacterial vehicle. Our recent studies have shown that combination therapies with siRNAs that target pro-oncogenic factors, and co-expressed tumor suppressor proteins comprise highly effective treatment strategies. However, development of suitable drug delivery systems is an equally important aspect of cancer therapy (Shao et al. 2010; Xu et al. 2009; Zhang et al. 2007, 2008). In this study, we constructed a plasmid containing both Stat3-shRNA and Endostatin cDNA (pEndo-Si-Stat3), and we used attenuated *Salmonella* to deliver the plasmid to an orthotopic model of prostate cancer (Fu et al. 1992; Hoffman 1999). The switch to an angiogenic phenotype in a tissue is dependent on the local balance between angiogenic stimulatory factors and inhibitors (Rastinejad 1989). Endostatin has been shown to be a better inhibitor of angiogenesis than Angiostatin (Chen et al. 1999). There is evidence that Endostatin blocks the binding of VEGF (Kim et al. 2002). Consistent with these observations, CD34 expression was decreased in tumor tissues expressing Endostatin, as demonstrated by immunohistochemistry (Fig. 3a, b). CD34 is expressed on small vessel endothelial cells and tumors of epithelial origin (Fina et al. 1990).

Intratumoral administration of naked plasmid DNA encoding mouse Endostatin has been shown to inhibit renal cell carcinoma growth (Zary and Zala 2001), and liposomes complexed with plasmids that encode Endostatin have been shown to inhibit breast tumor growth in mice when injected directly into tumors (Sacco et al. 2001). Adenovirus-mediated

systemic gene transfer of Endostatin was found to cause a significant reduction in tumor growth and to inhibit micrometastases in a mouse model (Sauter et al. 2000). Together, these studies indicate that targeting Endostatin directly in the tumor mass may cause tumor regression. However, these methods require direct intratumor instillation, tremendously limiting their practical utility in cancer therapy. In contrast, *Salmonella*-vectored therapies have been found to target tumor tissue preferentially.

Stat3 plays a key role in promoting prostate tumor proliferation in vitro and in vivo (Gao et al. 2005). The level of PCNA reflects the rate of cell proliferation and DNA synthesis (Strzalka and Ziemienowicz 2011). In the present study, immunohistochemical analyses showed that the control and pSi-Scramble groups expressed high levels of PCNA, which was robustly suppressed by pEndo-Si-Stat3 treatment (Fig. 2d, e). pEndo-Si-Stat3-treated tumors also showed significant apoptosis (Fig. 4). Stat3 activates several genes whose products promote cell cycle progression, for example *CCND1* or *MYC*, and prevent apoptosis, for example *BCL-2* (Gao et al. 2005). We also showed that combined expression of Endostatin and Si-Stat3 resulted in enhanced down-regulation of Bcl-2 (Fig. 4d–g). The silencing of Stat3 resulted in a down-regulation of both *Bcl-2* mRNA and protein with a corresponding increase in cancer cell apoptosis. Silencing of Stat3 also decreased both *VEGF* expression and angiogenesis (Fig. 3c–f). Thus, the anti-tumor effect of Endostatin is also mediated by the down-regulation of VEGF expression in tumor cells (Yang et al. 2011). Taken together, these studies suggest that the anti-tumor effects of Endostatin and Si-Stat3 may be attributed to decreased proliferation of both endothelial and tumor cells.

Endostatin is a 20-kDa inhibitor of angiogenesis that has recently been shown to inhibit the expression of VEGF, an angiogenic growth factor that is up-regulated by hypoxia via the HIF-1 transcription factor complex (Li et al. 2008; Liu et al. 2007; Passey 2006). Most human and rodent solid tumors have areas of hypoxia. Tumor hypoxia occurs because of the stochastic and slow development of the vasculature during tumor growth. The attenuated *Salmonella phoP/phoQ* strain has an excellent safety profile (Fields et al. 1986; Groisman et al. 1989; Miller et al. 1989; Thamm et al. 2005), displays a propensity to target tumors (Clairmont et al. 2000) and, being a facultative anaerobe, grows under hypoxic conditions.

In our recent report, a *phoP/phoQ* deletion mutant of *S. typhimurium* (Zhang et al. 2007) was employed as a carrier for siRNA or siRNA combined with a tumor suppressor for use in prostate cancer therapy. Regardless of the route of administration (i.e., oral, intravenous, intratumoral or intraperitoneal inoculation), *Salmonella*-delivered therapy resulted in significant anti-tumor effects with no evident toxicity in the mouse models (Kimura et al. 2010; Liu et al. 2010; Momiyama et al. 2012; Zhao et al. 2001, 2006, 2007). Our previous experimental findings and those of other reports (Tian et al. 2012; Pawelek et al. 1997; Low et al. 1999) show that attenuated *S. typhimurium* can specifically home to tumor cells, possibly via tumor-associated macrophages. The Endostatin and Si-Stat3 combination therapy also activates anti-tumor immune responses (Jia et al. 2012). Interestingly, in the current study, combined treatment with Endostatin and siRNA specific to Stat3 also activated various immune cells and cytokines (data not shown). Infiltration of CD4+ and CD8+ T lymphocytes into tumors was increased after pEndo-Si-Stat3 treatment. The functions of NK cells and T lymphocytes were enhanced. The number of CD8+ T lymphocytes was elevated, and the number of Treg cells was reduced. This combination therapy also increased the secretion of IFNγ and TNFα (inflammatory cytokines) and decreased the secretion of TGFβ1 (an immune-suppressing factor). Thus, the observed anti-tumor effects partially stem from essential changes in the anti-tumor immune response. Altogether, our data show that this combined therapy results in significant tumor regression and an improvement in animal survival.

In summary, a plasmid co-expressing both Si-Stat3 and Endostatin delivered via an attenuated *Salmonella* vector to prostate tumor cells causes more robust tumor suppression than observed with either individual treatment. This combined therapeutic approach results in a synergistic, multi-armed inhibition of tumor cell growth and provides a novel strategy to fight metastatic cancers, which are difficult to target and are resistant to most available therapies.

Acknowledgments

This work was funded by the National Natural Science Foundation of China (No. 30801354, No. 30970791 and No. 81201188) and the Jilin Provincial Science and Technology Department (Nos. 20080154). DVK is supported by the United States National Institutes of Health grants CA105005 and CA78282.

References

Beck MT, Peirce SK, Chen WY. Regulation of bcl-2 gene expression in human breast cancer cells by prolactin and its antagonist, hPRL-G129R. Oncogene. 2002; 21:5047–5055. [PubMed: 12140755]

Bromberg JF, Wrzeszczynska MH, Devgan G, Zhao Y, Pestell RG, Albanese C, Darnell JE. STAT3 as an oncogene. Cell. 1999; 98:295–303. [PubMed: 10458605]

Buettner R, Mora LB, Jove R. Activated STAT signaling in human tumors provides novel molecular targets for therapeutic intervention activated STAT signaling in human tumors provides novel molecular targets for therapeutic intervention 1. Clin Cancer Res. 2002; 8:945–954. [PubMed: 11948098]

Chen Q-R, Kumar D, Stass SA, Mixson AJ. Liposomes complexed to plasmids encoding angiostatin and endostatin inhibit breast cancer in nude mice. Cancer Res. 1999; 59:3308–3312. [PubMed: 10416583]

Clairmont C, Lee KC, Pike J, Ittensohn M, Low KB, Pawelek J, Bermudes D, Brecher SM, Margitich D, Turnier J, et al. Biodistribution and genetic stability of the novel antitumor agent VNP20009, a genetically modified strain of *Salmonella typhimurium*. J Infect Dis. 2000; 181:1996–2002. [PubMed: 10837181]

Fields PI, Swanson RV, Haidaris CG, Heffron F. Mutants of *Salmonella typhimurium* that cannot survive within the macrophage are avirulent. Proc Natl Acad Sci USA. 1986; 83:5189–5193. [PubMed: 3523484]

Fina L, Molgaard HV, Robertson D, Bradley NJ, Monaghan P, Delia D, Baker MA, Dc W, Fina BL, Molgaard HV, et al. Expression of the CD34 gene in vascular endothelial cells. Blood. 1990; 75:2417–2426. [PubMed: 1693532]

Fu X, Herrera H, Hoffman RM. Orthotopic growth and metastasis of human prostate carcinoma in nude mice after transplantation of histologically intact tissue. Int J Cancer. 1992; 52:987–990. [PubMed: 1459741]

Gao L, Zhang L, Hu J, Li F, Shao Y, Zhao D, Kalvakolanu DV. Down-regulation of signal transducer and activator of transcription 3 expression using vector-based small interfering RNAs suppresses growth of human prostate tumor in vivo. Clin Cancer Res. 2005; 11:6333–6341. [PubMed: 16144938]

Groisman EA, Chiao E, Lipps CJ, Heffront F. *Salmonella typhimurium* phoP virulence gene is a transcriptional regulator. Proc Natl Acad Sci USA. 1989; 86:7077–7081. [PubMed: 2674945]

Hoffman RM. Orthotopic metastatic mouse models for anticancer drug discovery and evaluation: a bridge to the clinic. Invest New Drugs. 1999; 17:343–359. [PubMed: 10759402]

Hohmann EL, Oletta CA, Killeen KP, Miller SI. phoP/phoQ-deleted *Salmonella typhi* (Ty800) is a safe and immunogenic single dose typhoid fever vaccine in volunteers. J Infect Dis. 1996; 173:1408–1414. [PubMed: 8648213]

Huang X, Wong MKK, Zhao Q, Gorelik E, Li M. Soluble recombinant endostatin purified from *Escherichia coli*: antiangiogenic activity and antitumor effect. Cancer Res. 2001; 61:478–481. [PubMed: 11212235]

Jia H, Li Y, Zhao T, Li X, Hu J. Antitumor effects of STAT3-shRNA and endostatin combined therapies, delivered by attenuated *Salmonella*, on orthotopically implanted hepatocarcinoma. Cancer Immunol Immunother. 2012; 61:1977–1987. [PubMed: 22527247]

Kamangar F. Patterns of cancer incidence, mortality, and prevalence across five continents: defining priorities to reduce cancer disparities in different geographic regions of the world. J Clin Oncol. 2012; 24:2137–2150. [PubMed: 16682732]

Kim Y-M, Hwang S, Kim Y-M, Pyun B-J, Kim T-Y, Lee S-T, Gho YS, Kwon Y-G. Endostatin blocks vascular endothelial growth factor-mediated signaling via direct interaction with KDR/Flk-1*. J Biol Chem. 2002; 277:27872–27879. [PubMed: 12029087]

Kimura H, Zhang L, Zhao M, Hayashi K, Tsuchiya H, Tomita K, Bouvet M, Wessels J. Targeted therapy of spinal cord glioma with a genetically modified *Salmonella typhimurium*. Cell Prolif. 2010; 43:41–48. [PubMed: 19922490]

Li X, Liu Y-H, Lee S-J. Prostate-restricted replicative adenovirus expressing human endostatin-angiostatin fusion gene exhibiting dramatic antitumor efficacy. Clin Cancer Res. 2008; 14:291–299. [PubMed: 18172281]

Liu F, Tan G, Li J, Dong X, Krissansen GW, Sun X. Gene transfer of endostatin enhances the efficacy of doxorubicin to suppress human hepatocellular carcinomas in mice. Cancer Sci. 2007; 98:1381–1387. [PubMed: 17627616]

Liu F, Zhang L, Hoffman RM, Zhao M. Vessel destruction by tumor-targeting *Salmonella typhimurium* A1-R is enhanced by high tumor vascularity. Cell Cycle. 2010; 9:4518–4524. [PubMed: 21135579]

Low KB, Ittensohn M, Le T, et al. Lipid A mutant *Salmonella* with suppressed virulence and TNFα induction retain tumor-targeting in vivo. Nat Biotechnol. 1999; 17:37–41. [PubMed: 9920266]

Miller SI, Kukral AM, Mekalanos JJ. A two-component regulatory system (phoP phoQ) controls *Salmonella typhimurium* virulence. Proc Natl Acad Sci USA. 1989; 86:5054–5058. [PubMed: 2544889]

Momiyama M, Zhao M, Kimura H, Bouvet M, Hoffman RM. Inhibition and eradication of human glioma with tumor-targeting *Salmonella typhimurium* in an orthotopic nude-mouse model. Cell Cycle. 2012; 11:628–632. [PubMed: 22274398]

Nam S, Buettner R, Turkson J, Kim D, Cheng JQ, Muehlbeyer S, Hippe F, Vatter S, Merz K-H, Eisenbrand G, Jove R. Indirubin derivatives inhibit STAT3 signaling and induce apoptosis in human cancer cells. PNAS. 2005; 102:5998–6003. [PubMed: 15837920]

Oshima K, Kawasaki H, Soda Y. Maxizymes and small hairpin-type RNAs that are driven by a tRNA promoter specifically cleave a chimeric gene associated with leukemia in vitro and in vivo. Cancer Res. 2003; 63:6809–6814. [PubMed: 14583478]

Passey S. Endostatin gene therapy inhibits tumour growth. Lancet Oncol. 2006; 7:199. [PubMed: 16538782]

Pawelek J, Low KB, Bermudes D. Tumor-targeted *Salmonella* as a novel anti-cancer vector. Cancer Res. 1997; 57:4537–4544. [PubMed: 9377566]

Rastinejad F. Regulation of the activity of a new inhibitor of angiogenesis by a cancer suppressor gene. Cell. 1989; 56:345–355. [PubMed: 2464438]

Real PJ, Sierra A, Juan AD, Segovia JC, Lopez-vega JM, Fernandez-luna JL. Resistance to chemotherapy via STAT3-dependent overexpression of Bcl-2 in metastatic breast cancer cells. Oncogene. 2002; 21:7611–7618. [PubMed: 12400004]

Ryan CJ, Wilding G. Angiogenesis inhibitors new agents in cancer therapy. Drugs Aging. 2000; 17:249–255. [PubMed: 11087003]

Sacco MG, Catò EM, Ceruti R, Soldati S, Indraccolo S, Caniatti M, Scanziani E, Vezzoni P. Systemic gene therapy with anti-angiogenic factors inhibits spontaneous breast tumor growth and metastasis in MMTVneu transgenic mice. Gene Ther. 2001; 8:67–70. [PubMed: 11402303]

Sauter BV, Martinet O, Zhang W-J, Mandeli J, Woo SLC. Adenovirus-mediated gene transfer of endostatin in vivo results in high level of transgene expression and inhibition of tumor growth and metastases. PNAS. 2000; 97:4802–4807. [PubMed: 10758166]

Shao Y, Liu Y, Shao C, Hu J, Li X, Li F, Zhang L, Zhao D, Sun L, Zhao X, et al. Enhanced tumor suppression in vitro and in vivo by co-expression of survivin-specific shRNA and wild-type p53 protein. Cancer Gene Ther. 2010; 17:844–854. [PubMed: 20706288]

Shichiri M, Hirata Y. Antiangiogenesis signals by endostatin. FASEB J. 2001; 15:1044–1053. [PubMed: 11292666]

Strzalka W, Ziemienowicz A. Proliferating cell nuclear antigen (PCNA): a key factor in DNA replication and cell cycle regulation. Ann Bot. 2011; 107:1127–1140. [PubMed: 21169293]

Thamm DH, Kurzman ID, King I, Li Z, Sznol M, Dubielzig RR, Vail DM, Macewen EG. Systemic administration of an attenuated, tumor-targeting *Salmonella typhimurium* to dogs with spontaneous neoplasia: phase I evaluation. Clin Cancer Res. 2005; 11:4827–4834. [PubMed: 16000580]

Tian Y, Guo B, Jia H, Ji K, Sun Y, Li Y, Zhao T, Gao L, Meng Y, Kalvakolanu DV, et al. Targeted therapy via oral administration of attenuated *Salmonella* expression plasmid-vectored STAT3-shRNA cures orthotopically transplanted mouse HCC. Cancer Gene Ther. 2012; 19:393–401. [PubMed: 22555509]

Weidner N, Folkman J, Pozza F, Allred EN, Moore DH, Meli S. Tumor angiogenesis: a new significant and early-stage breast carcinoma. J Natl Cancer Inst. 1992; 84:1875–1887. [PubMed: 1281237]

Xu D-Q, Zhang L, Kopecko DJ, Gao L, Shao Y, Guo B, Zhao L. Bacterial delivery of shRNAs: a new approach to solid tumor therapy. Methods Mol Biol. 2009; 487:161–187. [PubMed: 19301647]

Yang L, Lin Z, Lin J, Weng S. Antitumor effect of endostatin overexpressed in C6 glioma cells is associated with the down-regulation of VEGF. Int J Oncol. 2011; 38:465–471. [PubMed: 21165557]

Zary JS, Zala SS. Intra-tumoral administration of naked plasmid DNA encoding mouse endostatin inhibits renal carcinoma growth. Int J Cancer. 2001; 91:835–839. [PubMed: 11275988]

Zhang L, Gao L, Zhao L, Rnas P-BSI. Intratumoral delivery and suppression of prostate tumor growth by attenuated *Salmonella enterica* serovar *Typhimurium* carrying plasmid-based small interfering RNAs. Cancer Res. 2007; 67:5859–5864. [PubMed: 17575154]

Zhang L, Gao L, Li Y, Lin G, Shao Y, Ji K, Yu H, Hu J. Effects of plasmid-based STAT3-specific short hairpin RNA and GRIM-19 on PC-3 M tumor cell growth GRIM-19 on PC-3 M tumor cell growth. Clin Cancer Res. 2008; 14:559–568. [PubMed: 18223232]

Zhao M, Yang M, Baranov E, Wang X, Penman S, Moossa AR, Hoffman RM. Spatial-temporal imaging of bacterial infection and antibiotic response in intact animals. PNAS. 2001; 98:9814–9818. [PubMed: 11481427]

Zhao M, Yang M, Ma H, Yang Z, Hoffman RM. Targeted therapy with a *Salmonella typhimurium* leucine-arginine auxotroph cures orthotopic human breast tumors in nude mice. Cancer Res. 2006; 66:7647–7652. [PubMed: 16885365]

Zhao M, Geller J, Ma H, Yang M, Penman S, Hoffman RM. Monotherapy with a tumor-targeting mutant of *Salmonella typhimurium* cures orthotopic metastatic mouse models of human prostate cancer. PNAS. 2007; 104:10170–10174. [PubMed: 17548809]

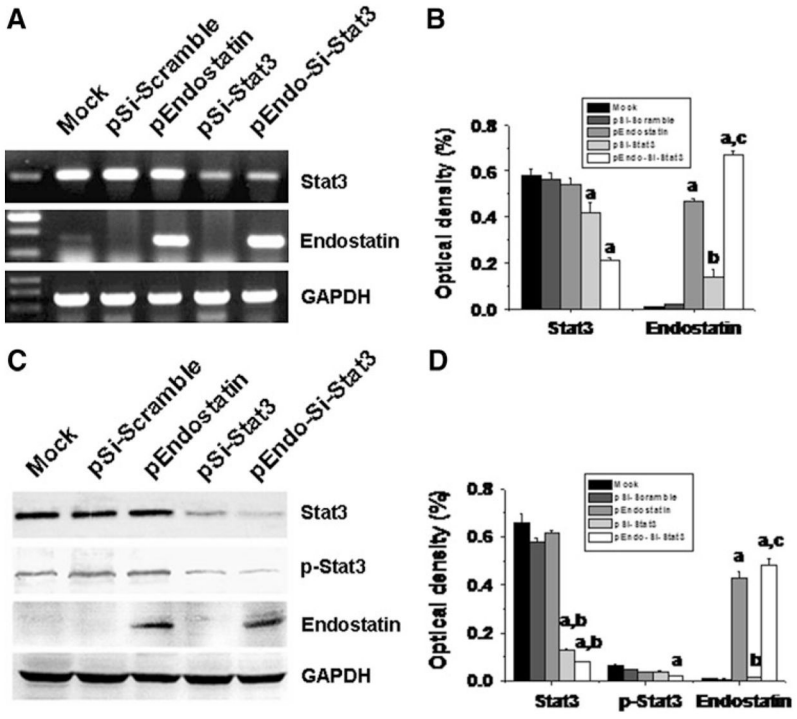

Fig. 1.

Effects of *Salmonella*-delivered plasmids on the expression of Stat3, p-Stat3 and Endostatin. **a** Expression of Endostatin and Stat3 mRNA as measured by RT-PCR following the indicated treatments. **b** Densitometric quantification of the RT-PCR from **a. c** Western blot analyses of Stat3, p-Stat3 and Endostatin expression following the indicated treatments. **d** Densitometric quantification of the Western blot analysis from **c**. *a* $P < 0.05$ versus the Mock or Si-Scramble group; *b* $P < 0.05$ versus the Endostatin group; *c* $P < 0.05$ versus the Si-Stat3 group

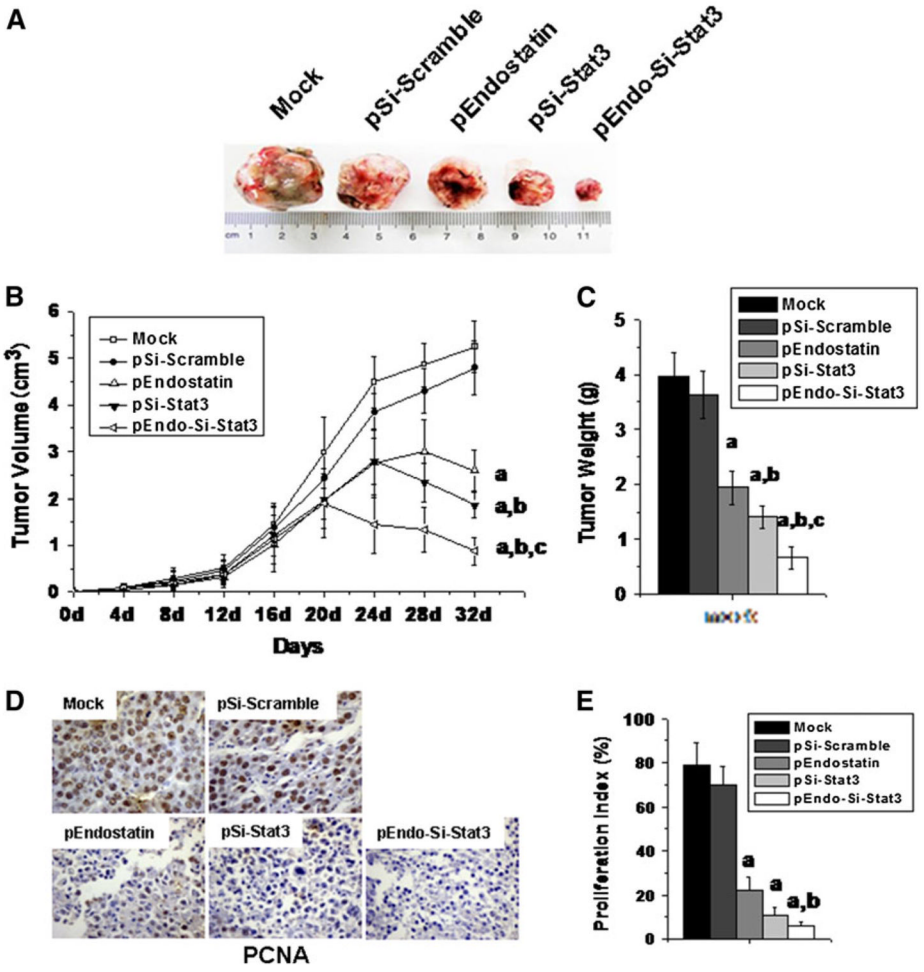

Fig. 2.

Effects of various plasmids on tumor proliferation. **a** Representative isolated tumors from the Mock-, Si-Scramble-, Endostatin-, Si-Stat3- and Endo-Si-Stat3-treated mice were collected when tumor-bearing mice were killed at day 32 post-treatment. **b** Tumor growth curves over 32 days following treatments were created based on the tumor sizes measured every fourth day. $n = 8$. Mean ± SD. $^{*}P < 0.05$ versus tumor; $^{**}P < 0.01$ versus tumor. **c** Wet tumor weights were measured when the animals were killed at day 32 post-treatment. **d** Immunohistochemical staining of PCNA (magnification of ×400) was performed on tumor tissue obtained at day 32 following the indicated treatments. **e** Semi-quantitative analysis of PCNA expressed as the proliferation index (PI) following the indicated treatments. *a* $P < 0.05$ versus the Mock or Si-Scramble group; *b* $P < 0.05$ versus the Endostatin group; *c* $P < 0.05$ versus the Si-Stat3 group

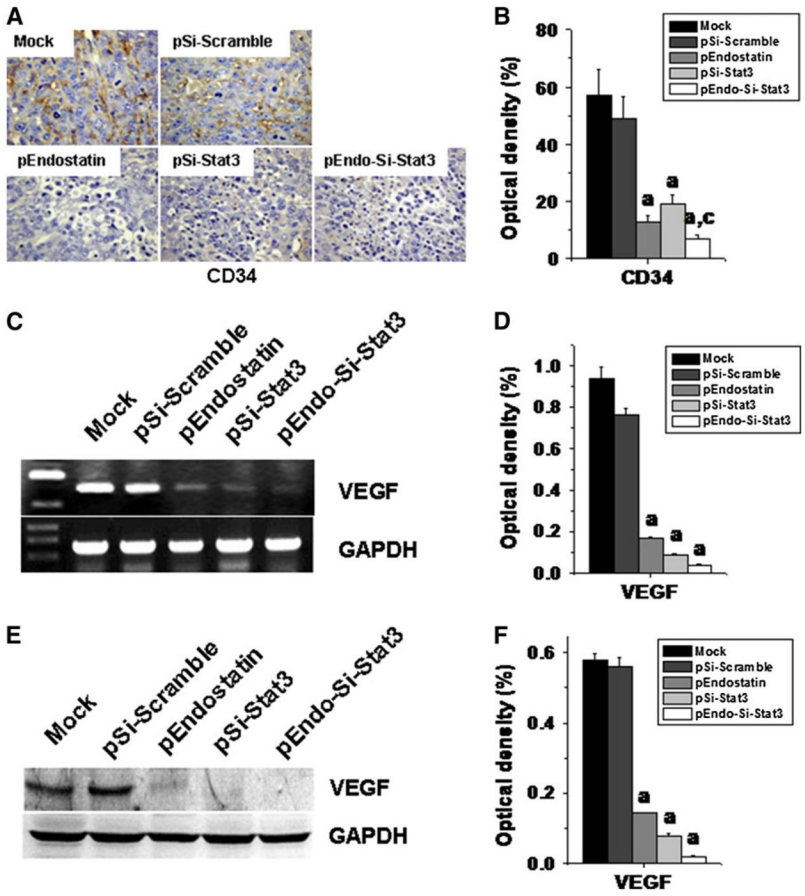

Fig. 3.

Tumor microvascular density and VEGF mRNA and protein levels following different plasmid treatments. **a** Immunohistochemical analysis of CD34 (×400 mag.), reflecting the distribution of blood vessels in tumor tissues from the indicated treatment groups. **b** Semi-quantitative analysis of CD34 expression. **c** Tumor VEGF mRNA expression measured by RT-PCR following the indicated treatments. **d** Densitometric quantification of the VEGF RT-PCR from **c. e** Western blot analyses of VEGF protein expression in tumors following the indicated treatments. **f** Quantification of the Western blot data from **e**. *a* $P < 0.05$ versus the Mock or Si-Scramble group; *b* $P < 0.05$ versus the Endostatin group; *c* $P < 0.05$ versus the Si-Stat3 group

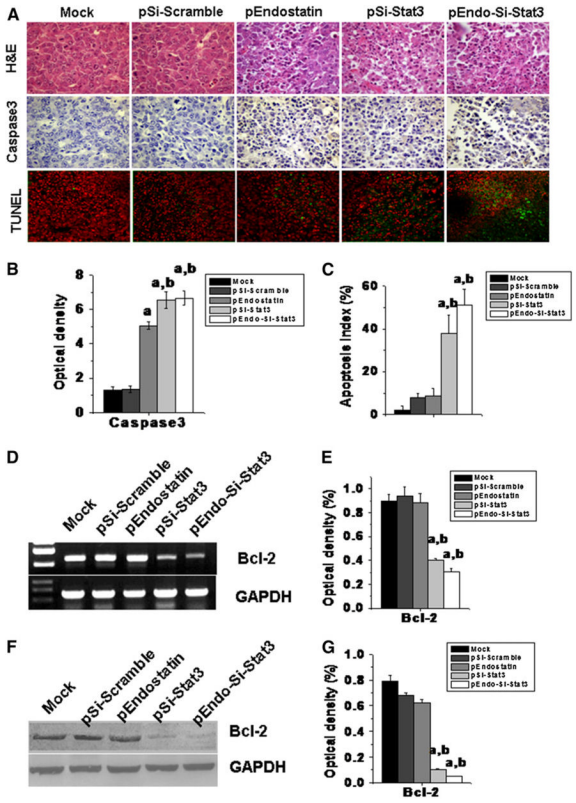

Fig. 4.

Effects of treatment on the induction of apoptosis and Bcl-2 expression in tumors. **a** H&E staining, immunohistochemical staining for Caspase3 (×400 mag.) and TUNEL staining (×400 mag.) were performed on tumor tissue obtained from mice following the indicated treatments. **b** Quantification of the Caspase3 expression from **a. c** Semi-quantitative analysis of TUNEL staining, expressed as apoptotic index (AI). **d** Bcl-2 mRNA levels in treated tumors, as measured by RT-PCR. **e** Densitometric quantification of Bcl-2 mRNA levels from **d**, standardized to GAPDH. **f** Western blot analyses of Bcl-2 protein expression in treated tumors. **g** Quantification of the Bcl-2 Western blot analysis from **f**, standardized to GAPDH. *a* P <0.05 versus the Mock or Si-Scramble group; *b* P < 0.05 versus the Endostatin group; *c* P <0.05 versus the Si-Stat3 group